B. DYBOWSKI*,#, J. SZYMSZAL**, Ł. POLOCZEK**, A. KIEŁBUS*

INFLUENCE OF THE CHEMICAL COMPOSITION ON ELECTRICAL CONDUCTIVITY AND MECHANICAL PROPERTIES OF THE HYPOEUTECTIC Al-Si-Mg ALLOYS

Due to low density and good mechanical properties, aluminium alloys are widely applied in transportation industry. Moreover, they are characterized by the specific physical properties, such as high electrical conductivity. This led to application of the hypoeutectic Al-Si-Mg alloys in the power generation industry. Proper selection of the alloys chemical composition is an important stage in achievement of the demanded properties. The following paper presents results of the research on the influence of alloys chemical composition on their properties. It has been revealed that Si and Ti addition decreases electrical conductivity of the Al-Si-Mg alloys, while Na addition increases it. The mechanical properties of the investigated alloys are decreased by both silicon and iron presence. Sodium addition increases ductility of the Al-Si-Mg alloys.

Keywords: hypoeutectic Al-Si-Mg alloys, sand casting, electrical conductivity, mechanical properties, chemical composition.

1. Introduction

Aluminium alloys are one of the lightest structural materials. With density equal about $2.7 g/cm^3$, they are more and more often applied in the automotive and aerospace industries. They are also characterized by the good mechanical properties and corrosion resistance [1, 2]. As they possess good technological properties (castability, deformability), aluminium alloys may be formed into the complicated elements, such as e.g. engine blocks [3]. Moreover, their physical properties, such as high electrical conductivity led to the application of the aluminium alloys in the power generation industry. One of such elements are the parts of the gas insulated switchgears. These are usually large, thick-walled, sand cast elements with required high electrical conductivity and hardness. The demanded properties may be obtained only after careful selection of the alloys chemical composition. Hypoeutectic Al-Si alloys with Mg addition are commonly applied for the elements dedicated for power generation industry.

Silicon is known to improve casting properties of the aluminium alloys. Si decreases their volumetric shrinkage and increases fluidity. However, increasing Si content leads to the formation of more dispersed microshrinkages, evenly distributed within the alloys microstructure [4, 5]. Silicon is said to increase the mechanical properties of the hypoeutectic Al-Si alloys. This is often attributed to the modification of morphology and type of the Fe-rich intermetallic phases. On the other hand – in the low iron alloys, increasing Si content may decrease ductility and tensile strength [6].

Magnesium is added to the Al-Si alloys to induce age hardening response by the precipitation of Mg-Si or Al-Mg-Si intermetallic phases [7]. It also influences formation of Fe-bearing phases, leading to the precipitation of π-AlFeMgSi phase rather than β-AlFeSi [8]. Mg addition increases slightly tensile strength of the aluminium alloys. Unfortunately, due to formation of massive, brittle π phase, loss of their ductility is also observed [9]. Moreover, magnesium decreases electrical conductivity of the aluminium alloys [10].

The most harmful impurity in Al-Si casting alloys is iron. Fe leads to the formation of many intermetallic phases, depending on the chemical composition of the alloy and its solidification rate [11÷13]. The most detrimental for the properties of the Al-Si alloys is β-Al_5FeSi phase with platelet-like morphology. Slow cooling rates favours formation of this phase [14] before the last stages of solidification of α-Al+β-Si eutectic. This leads to the increased interdendritic porosity [15]. Large, brittle precipitates decrease alloys ductility and their impact strength [16].

Silicon tends to formation of large, interconnected platelet-like crystals during the solidification. This morphology may be changed by the chemical modification of the Al-Si alloys with elements such as Na, Sr or Sb [17, 18]. Their addition leads to formation of fine, fibrous eutectic mixture, increasing alloys ductility. The microstructure modification increases also alloys electrical conductivity. Titanium addition refines the α-Al dendrites, however it strongly decreases aluminium electrical conductivity [19].

The following paper presents results of the investigations on the influence of the chemical composition of hypoeutectic Al-Si alloys on their mechanical properties and electrical conductivity. The alloying elements content varied in the range allowed by the PN-EN 1706 and Siemens L42/04 specifications.

* SILESIAN UNIVERSITY OF TECHNOLOGY, INSTITUTE OF MATERIALS SCIENCE, 8 KRASIŃSKIEGO STR., 40-019 KATOWICE, POLAND

** SILESIAN UNIVERSITY OF TECHNOLOGY, DEPARTMENT OF PRODUCTION ENGINEERING, 8 KRASIŃSKIEGO STR., 40-019 KATOWICE, POLAND

Corresponding author: dybowski.bartlomiej@gmail.com

2. Research material and methodology

Material for the research consisted of three hypoeutectic aluminium-silicon casting alloys. These were AlSi5Mg, AlSi7Mg and AlSi9Mg alloys. Several melts were prepared for the research. Chemical composition of the obtained materials varied in the ranges acceptable by the PN-EN 1706 and Siemens L42/04 specifications. The particular attention was given to varying content of alloying elements and impurities such as Si, Mg, Ti and Na (Tab. 1). The alloys were sand cast in form of the tensile testing specimens (Fig. 1). One specimen from each melt was cut for the metallographic investigations, while the other three specimens were used for tensile testing.

The specimens for the metallographic investigations were cut from the middle of the castings. Microsections preparation included grinding on the SiC abrasive papers with grades 120÷2500 and polishing on diamond suspensions with the mean grain size 6 μm, 3 μm and 1 μm. Final polishing step was done on Struers Op-U colloidal silica suspension with the grain size 0.05 μm. The alloys porosity was evaluated on the un-

etched microsections, while microstructure was observed on the microsections etched in Keller's reagent (190 ml H_2O, 5 ml HNO_3, 3 ml HCl and 2 ml HF). The microstructure observations were conducted on Olympus GX71 light microscope (LM) as well as Hitachi S3400N scanning electron microscope (SEM), equipped with energy dispersive X-Ray spectrometer (EDS).

The quantitative evaluation of the alloys porosity has been conducted on 15 images recorded with magnification 50x. The evaluation was done on un-etched specimens. Detection and measurement were conducted in the MetIlo software.
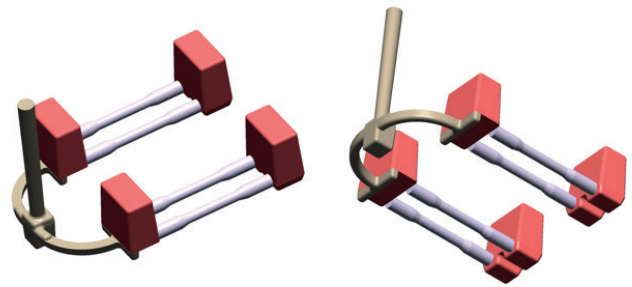

Fig. 1. Pattern of the specimens cast for the research

TABLE 1

Chemical composition of the prepared alloys (wt. %)

	Si	Fe	Cu	Mn	Mg	Zn	Ti	Na	Al
AlSi5Mg Siemens L42/04	4.5÷7.5	0.15	0.01	0.015	0.3÷0.4	0.07	0.01	-	Bal.
AlSi5Mg – 1	4.84	0.145	0.002	0.007	0.342	0.005	0.007	0.0028	Bal.
AlSi5Mg – 2	6.11	0.160	0.003	0.009	0.302	0.006	0.008	0.0002	Bal.
AlSi5Mg – 3	4.97	0.140	0.002	0.007	0.308	0.004	0.008	0.0	Bal.
AlSi5Mg – 4	5.13	0.140	0.002	0.007	0.419	0.005	0.008	0.0	Bal.
AlSi5Mg – 5	5.03	0.129	0.002	0.007	0.398	0.005	0.008	0.0029	Bal.
AlSi5Mg – 6	5.00	0.154	0.002	0.008	0.400	0.006	0.007	0.0065	Bal.
AlSi7Mg PN-EN1706	6.5-7.5	0.19	0.05	0.10	0.25-0.45	0.07	0.25	-	Bal.
AlSi7Mg – 1	7.02	0.099	0.004	0.002	0.258	0.003	0.099	0.0031	Bal.
AlSi7Mg – 2	7.03	0.097	0.004	0.002	0.25	0.003	0.102	0.0008	Bal.
AlSi7Mg – 3	6.86	0.097	0.003	0.003	0.399	0.005	0.107	0.0007	Bal.
AlSi7Mg – 4	6.97	0.090	0.003	0.003	0.322	0.006	0.102	0.0032	Bal.
AlSi7Mg – 5	6.97	0.101	0.004	0.003	0.337	0.006	0.109	0.0057	Bal.
AlSi7Mg – 6	6.84	0.091	0.004	0.003	0.271	0.006	0.232	0.003	Bal.
AlSi7Mg – 7	6.95	0.091	0.004	0.010	0.258	0.006	0.400	0.002	Bal.
AlSi9Mg PN-EN1706	9.0÷11.0	0.55	0.10	0.45	0.20÷0.45	0.10	0.15	-	Bal.
AlSi9Mg – 1	9.42	0.101	0.002	0.009	0.348	0.003	0.111	0.0	Bal.
AlSi9Mg – 2	10.46	0.097	0.008	0.007	0.244	0.005	0.116	0.0011	Bal.
AlSi9Mg – 3	9.32	0.099	0.002	0.009	0.345	0.003	0.113	0.0	Bal.
AlSi9Mg – 4	9.01	0.079	0.002	0.007	0.370	0.004	0.127	0.0	Bal.
AlSi9Mg – 5	9.41	0.084	0.002	0.008	0.339	0.004	0.114	0.0049	Bal.
AlSi9Mg – 6	9.37	0.098	0.002	0.009	0.418	0.004	0.109	0.0079	Bal.

Electrical conductivity of the alloys was measured with an eddy-current Sigmatest 2.069 tester. The measurements were done on the un-etched specimens for the metallographic observations. Eight measurements were conducted for each melt. Mechanical properties of the alloys were measured in the tensile tests done on ZWICK 1474 tensile testing machine. The properties were investigated on three specimens from each melt. The influence of the alloying elements on the alloys properties was statistically evaluated.

3. Research results

3.1. Microstructure

The microstructure of the investigated alloys consists mainly of α-Al solid solution dendrites and α-Al+β-Si binary eutectic mixture. Silicon crystals possess different morphologies, depending on the Na content. With increasing Na content, morphology of eutectic Si is changed from the massive, interconnected platelets to the colonies of fine, also interconnected fibrous crystals (Fig. 2).
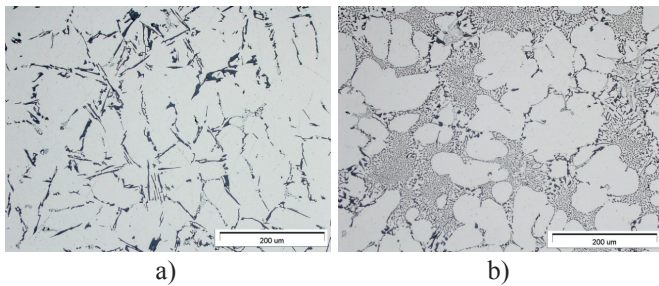

a)   b)

Fig. 2. Eutectic silicon morphology in AlSi7Mg alloy, un-etched, LM; a) 0.0007 wt. % Na; b) 0.0057 wt.% Na

Some intermetallic phases are also observed within the Al-Si-Mg alloys microstructure. These are: Chinese script-like Mg_2Si phase with FCC crystal structure, π-$Al_9FeMg_3Si_5$ phase with hexagonal structure, blocky, cubic $Al_{17}(Fe_{3.2} Mn_{0.8})_3Si_2$ phase and needle-like phase, the most probably monoclinic β-Al_5FeSi phase (Fig. 3). Fine, rod-like and globular phases are also observed within the α-Al solid solution dendrites. As previous investigations shown, the rod-like precipitates are metastable Al-Mg-Si phases (U1 and probably U2), while the globular particles are the most probably fine Si crystals. The phases analysis were published before [20].

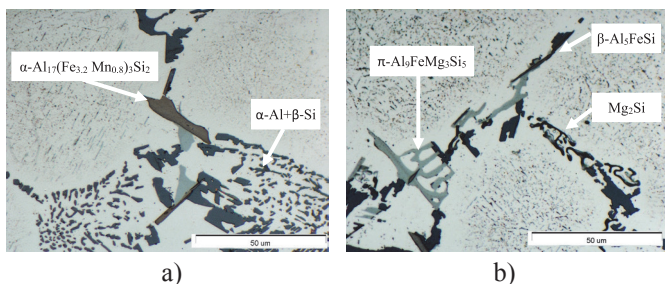a)   b)

Fig. 3. Intermetallic phases in the AlSi5Mg alloy's microstructure, Keller's etch, LM

Moreover, some needle like phases after etching revealed inhomogeneous structure (Fig. 4a) – which may indicate that the particles are formed by the two different phases. EDS analysis of a few such particles revealed differences in the chemical composition of above mentioned regions. The internal regions of the particles contain about 50 at.% of Al, 29 at.% of Si, 20 at.% of Fe, and about 1 at.% of Mn (Fig. 4b, Tab. 2). The external parts of the particles consist of about 62 at.% of Al, 18-19 at.% of Si as well as Fe and about 1 at. % of Mn (Fig. 4b, Tab. 2).

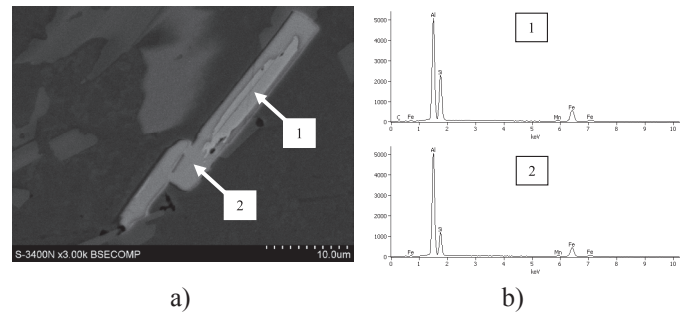a)   b)

Fig. 4. Inhomogeneous etching of Fe-bearing particle, Keller's etch, SEM (a) and corresponding to the indicated points EDS charts (b)

TABLE 2

Chemical composition of the intermetallic phases shown in the Fig. 4 (at. %)

	Al	Si	Mn	Fe
Fig. 4, pt. 1	50.9	28.2	0.8	20.1
Fig. 4, pt. 2	61.8	18.3	1.1	18.9

3.2. Electrical conductivity and mechanical properties

Results of the electrical conductivity and mechanical properties of the investigated alloys are given in the Tab. 3.

3.3. Multiple regression

Influence of the chemical composition on the electrical conductivity and mechanical properties of the investigated alloys has been evaluated statistically. Multiple linear regression analysis were done with the backward elimination approach for the evaluation of the strength and direction of interactions between variables (alloying elements) and the properties. After each elimination step, residual analysis were done for validation of estimated models. It has to be mentioned, that estimated models may be applied for the properties prediction only in the investigated ranges of the alloying elements content. These are: Si: 4.84-10.46 wt. %; Mg: 0.244-0.419 wt. %; Fe: 0.079-0.160 wt. %; Ti: 0.007- 0.4 wt. %; Na: 0-0.008 wt. %.

3.3.1 Electrical conductivity

In the first step of the analysis, influence of magnesium content on the conductivity has been eliminated (probability p=0.785), in the second stage – iron content has been

TABLE 3

Electrical conductivity and mechanical properties of the investigated alloys

Alloy	Varying element	Electrical conductivity σ [MSm-1]	Ultimate tensile strength UTS [MPa]	Yield strength YS [MPa]	Elongation A5 [%]
AlSi5Mg					
AlSi5Mg – 1	Min. Si	24.54±0.19	158±2	97±1	5.1±0.2
AlSi5Mg – 2	Max. Si	22.7±0.07	149±2	96±1	2.9±0.2
AlSi5Mg – 3	Min. Mg	22.98±0.03	155±4	97±4	3.9±0.5
AlSi5Mg – 4	Max. Mg	22.81±0.06	153±12	107±2	2.5±1.1
AlSi5Mg – 5	Min. Na	24.55±0.06	165±1	104±1	4.9±0.3
AlSi5Mg – 6	Max. Na	24.51±0.06	159±2	99±1	4.5±0.4
AlSi7Mg					
AlSi7Mg – 1	Mean Si	21.51±0.72	168±4	112±1	3.3±0.4
AlSi7Mg – 2	Min. Mg	20.02±0.12	160±1	112±1	2.2±0.1
AlSi7Mg – 3	Max. Mg	20.04±0.06	173±2	126±4	2.2±0.1
AlSi7Mg – 4	Min. Na	21.7±0.1	172±6	129±11	2.4±0.1
AlSi7Mg – 5	Max. Na	21.92±0.1	172±3	119±5	3.1±0.8
AlSi7Mg – 6	Min. Ti	20.67±0.03	175±5	118±5	3.4±0.2
AlSi7Mg – 7	Max. Ti	19.97±0.09	173±5	119±9	2.9±0.3
AlSi9Mg					
AlSi9Mg – 1	Min. Si	18.24±0.05	155±1	106±4	1.9±0.1
AlSi9Mg – 2	Max. Si	17.48±0.05	136±21	108±3	1.1±1.1
AlSi9Mg – 3	Min. Mg	18.28±0.06	160±5	108±5	2.5±0.3
AlSi9Mg – 4	Max. Mg	18.58±0.02	168±1	116±1	2.7±0.1
AlSi9Mg – 5	Min. Na	20.39±0.12	164±0	106±2	3.0±0.1
AlSi9Mg – 6	Max. Na	20.89±0.18	163±4	101±2	3.5±0.4

eliminated (p=0.3878). Other three variables (Si content – $p<0.0001$, Ti content – $p=0.0166$ and Na content – $p<0.0001$) have statistically significant influence on the Al-Si-Mg alloys electrical conductivity. Silicon and titanium content decrease the property, while Na content significantly increases. The electrical conductivity is given with equation (1), R^2 coefficient of determination for this model is equal 0.9303. Normal probability plot of residuals (Fig. 5) proves effectiveness of the evaluated model.

$$\sigma = 28.709 - 1.026 \times Si - 6.837 \times Ti + 342.998 \times Na \quad (1)$$

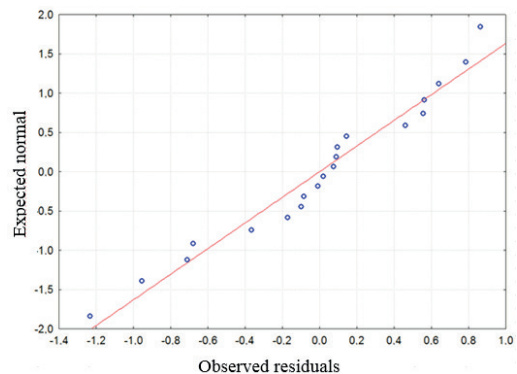where: σ is the electrical conductivity, MS/m; Si, Ti and Na are alloying elements contents, wt. %.

Fig 5. Normal probability plot of residuals for the electrical conductivity prediction model (1)

3.3.2 Ultimate Tensile Strength

Na content has been eliminated during the first step of analysis (p=0.1197), followed by elimination of Ti content (p=0.0836). Other factors (Si content – p<0.0001, Mg content – p=0.0107 and Fe content – p<0.0001) are statistically significant in prediction of alloys UTS. Silicon and iron content decreases alloys mechanical properties, while magnesium addition increases it. The UTS is given with equation (2), R^2 coefficient of determination for this model is equal 0.7452. Normal probability plot of residuals (Fig. 6) proves effectiveness of the evaluated model.

$$UTS = 235.565 - 5.278 \times Si + 47.820 \times Ti - 469.696 \times Fe \quad (2)$$

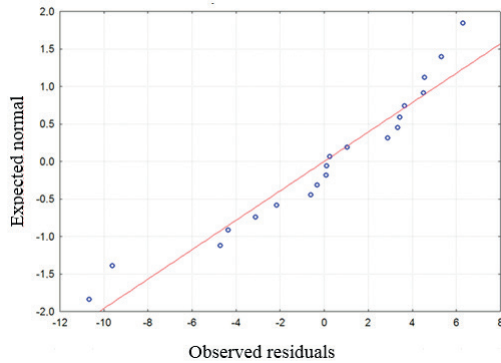where: UTS is the ultimate tensile strength, MPa; Si, Ti and Fe are alloying elements contents, wt. %

Fig. 6. Normal probability plot of residuals for the UTS prediction model (2)

3.3.3 Yield strength

In the case of yield strength prediction, more factors were eliminated. Firstly, magnesium content has been eliminated (p=0.4625). Secondly Ti content (p=0.6028) and Na content (p=0.4781) were removed from the model. Addition of both silicon (p=0.0092) as well as iron (p<0.0001) decrease yield strength of Al-Si-Mg alloys. The change of YS is given with relationship (3). R^2 coefficient of determination for this equation is equal 0.6528, normal probability plot of residuals (Fig. 7) proves effectiveness of the evaluated model.

$$YS = 174.197 - 2.842 \times Si - 406.036 \times Fe \quad (3)$$

where: YS is the yield strength, MPa; Si and Fe are alloying elements contents, wt. %.
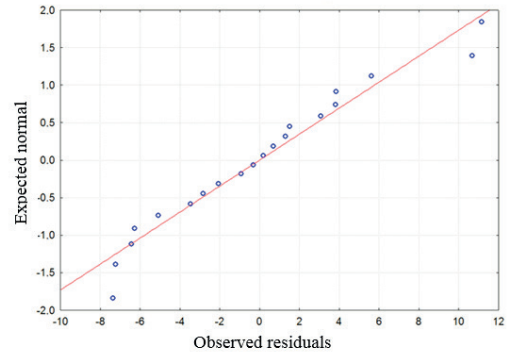

Fig. 7. Normal probability plot of residuals for the YS prediction model (3)

3.3.4 Elongation

Proper model of elongation prediction is also dependant on two variables. In the first stage, Ti content has been removed (p=0.9210), followed by elimination of Mg (p=0.6471) and Fe (p=0.5052). Silicon content (p=0.0003) decreases alloys elongation, while addition of Na (p=0.0059) increases the property. Relationship between Si and Na content and alloys elongation is given with equation (4). R^2 coefficient of determination for this model is equal 0.6039, normal probability plot of residuals (Fig. 8) proves effectiveness of the evaluated model.

$$A_5 = 5.251 - 0.3688 \times Si + 189.811 \times Na \quad (4)$$

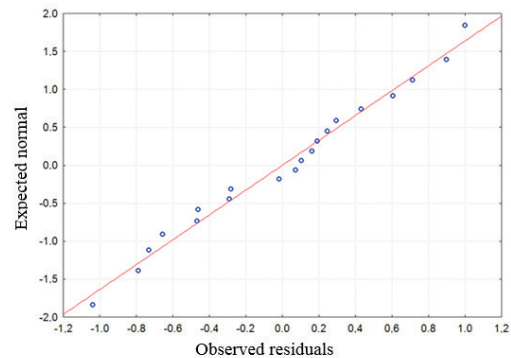where: A5 is the elongation, %; Si and Na are alloying elements contents in wt. %.

Fig. 8. Normal probability plot of residuals for the A5 prediction model (4)

3.3.5 Model for the chemical composition optimization

As each of the investigated properties should be as high as it is possible, similar multiple regression method might have been applied for the optimization of Al-Si-Mg alloys chemical composition. The independent variable was equal to the sum of standardized values of each investigated property. The standardized values are estimated according to the equation (5), and are dimensionless. Standardization allows for addition

of the properties, which, at the beginning possessed different dimensions.

$$X_S = \frac{X_E - \overline{X}}{S} \qquad (5)$$

where, X_S is a standardized value, X_E is an empirical value, $\overline{X}$ is a mean value and S is a standard deviation.

During the backwards elimination, Ti content influence has been removed at first (p=0.1191). Similarly, Mg influence has been eliminated (p=0.1994). Addition of Si (p<0.0001) and Fe (p<0.0001) decrease the final property, while Na addition (p=0.0065) is beneficial. The relationship between Si, Na and Fe content and final property is given with equation (6). R_2 coefficient of determination for this model is equal 0.8577, normal probability plot of residuals (Fig. 9) proves effectiveness of the evaluated model.

$$F = 23.156 - 1.797 \times Si - 102.363 \times Fe + 333.485 \times Na \quad (6)$$

where: F is the sum of standardized values of the investigated properties; Si, Fe and Na are alloying elements contents, wt. %.
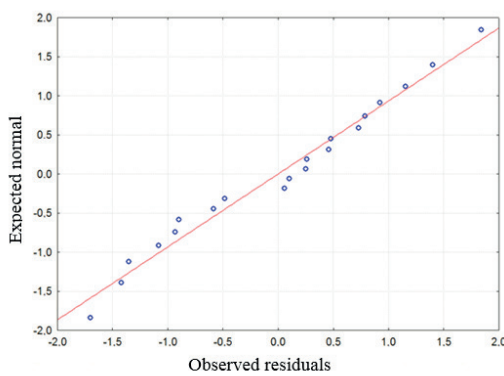

Fig. 9. Normal probability plot of residuals for the F prediction model (6)

4. Discussion

The microstructure of the hypoeutectic Al-Si-Mg alloys id formed by the α-Al solid solution dendrites and binary α-Al+β-Si eutectic mixture. Na-modification leads to change in the eutectic silicon morphology from the interconnected platelets to the fine, fibrous crystals. Several intermetallic phases are also observed in the alloys microstructure. These are blocky $Al_{17}(Fe_{3.2}\ Mn_{0.8})_3Si_2$, irregular π-$Al_9FeMg_3Si_5$, Chinese script-like Mg_2Si and needle-like Fe-bearing phase, probably Al_5FeSi. Moreover, within the structure of some needle- or platelet-like particles, two different regions are easily distinguishable. The internal region - enriched in Si (29 at.%) and Fe (20 at.%) has irregular shape, while the external region with Fe/Si ratio equal to 1:1 possess regular shape with straight edges. Similar phenomena has been observed before. Gorny et al. [14] have found that in AlSi7(Fe) alloy some particles of the τ_5 (α-Al_8Fe_2Si) are enveloped by the τ_6 (β-$Al_9Fe_2Si_2$) phase. The τ_5 phase undergoes peritectic reaction, which may not be completed. However, chemical composition of the phase found during the research, does not match any of the suggested compositions. It is the closest to the chemical composition of δ-Al_3(Fe, Mn)Si_2 phase, found often in the high silicon and iron aluminium alloys [21, 22]. Such phase is also said to undergo peritectic reaction into the β-phase [22]. As the casting solidification is not an equilibrium phenomenon, δ-Al_3(Fe, Mn)Si_2 may probably also be formed in the alloys with lower silicon and iron contents and may not undergo complete transformation to the more stable, β-phase. The fine phases observed within the α-Al dendrites are formed during slow cooling in the sand mould. The mechanism may be similar to the precipitation of lamellar $Mg_{17}Al_{12}$ phase from the supersaturated regions of α-Mg solid solution in the aluminium containing magnesium alloys [23, 24]. In contrast, in the investigated case the precipitation process is observed in the whole volume of dendrites.

All estimated dependences between the alloys chemical composition and their properties are statistically significant. Comparison of the experimental and predicted values (Fig. 10) shows good agreement, particularly in the case of the electrical conductivity, where the dependence is nearly linear. However, it has to be remembered, that the estimated models are correct only within the range of investigated alloys compositions: Si: 4.84-10.46 wt. %; Mg: 0.244-0.419 wt. %; Fe: 0.079-0.160 wt. %; Ti: 0.007- 0.4 wt. %; Na: 0-0.008 wt. %.
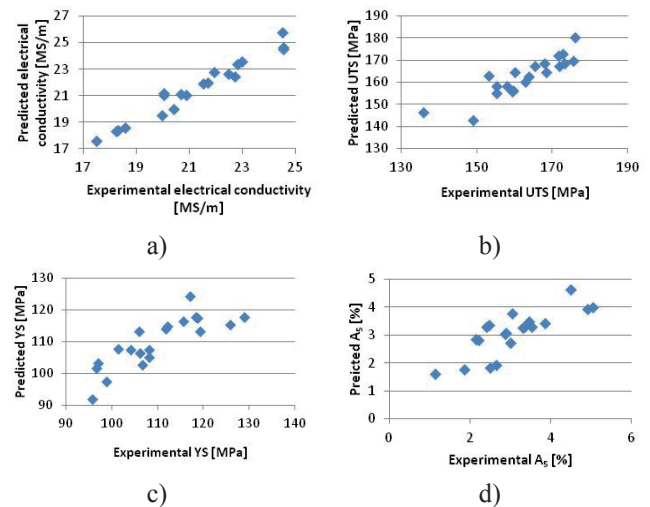

a)

b)

c)

d)

Fig. 10. Comparison of predicted and experimental properties of the Al-Si alloys; a) Electrical conductivity; b) UTS; c) YS; d) Elongation

The electrical conductivity of the hypoeutectic Al-Si alloys depends mainly on the Si, Ti and Na content. Increase of Si and Ti content decreases the conductivity, while degree of modification (Na-content) strongly increases. The electrical conductivity depends mainly on the state of α-Al matrix (degree of saturation with alloying elements, residual stresses etc.) as well as presence of obstacles such as other phase's particles, porosity, grain boundaries etc. Mamala et al. [10] have found that iron strongly affects the conductivity of the α-Al solid solution, however it is not so harmful when bounded outside the solid solution. This conclusion is in accordance with our investigations, in which iron is present mainly in form of intermetallic phases and is not determining for the electrical properties. Unlike Fe, silicon is also harmful when is precipitated outside the solid solution.

Its deleterious effect on the electrical conductivity of the Al-Si alloys has already been confirmed [25]. Na addition increases this property by changing the morphology of eutectic Si into the fine, fibrous crystals.

Both the yield strength and ultimate tensile strength are decreased by the increasing Si content. Silicon is generally said to increase the Al-Si mechanical properties, however in the case of low magnesium and low iron alloys, the silicon addition may decrease both their tensile strength and ductility [6]. This is in accordance with the conducted investigations, in which increasing Si content reduces the alloys mechanical properties. It may also be attributed to the increasing volume fraction of the alloys porosity. With the increasing porosity alloys mechanical properties decrease [5, 26]. The addition of silicon suppress formation of significant volumetric shrinkage, however, it leads to the increase of microshrinkages, evenly distributed within the whole volume of the material. When the silicon content approaches the eutectic composition, formation of less homogenously distributed, big pores is more probable [4]. Evaluation of the porosity in the investigated alloys, revealed that highest volume fraction of pores in the case of AlSi5Mg alloy was equal to 0.481%, with mean area of pore flat section equal to 0.0013 mm^2. In the case of AlSi9Mg alloy, the highest porosity was equal to 1.56% with mean pore flat section nearly four times higher – 0.0048 mm^2. Increasing iron content also leads to decrease in the alloys mechanical properties, which is attributed to formation of large, brittle intermetallic phases – mainly β-Al$_5$FeSi phase.

The achievement of the highest possible electrical conductivity and mechanical properties demands small contents of both silicon (affecting each property) and iron (strongly affecting mechanical properties). On the other hand, increasing Na content (degree of modification) is beneficial for both electrical conductivity and ductility of the material. Final model of chemical composition optimization does not include titanium content. However, as the titanium affects strongly electrical conductivity, its content should also be lowered.

5. Conclusions

1. Hypoeutectic Al-Si-Mg alloys microstructure consists of α-Al solid solution dendrites and binary α-Al+β-Si eutectic mixture. Moreover, intermetallic phases such as Mg$_2$Si, π-Al$_9$FeMg$_3$Si$_5$, α-Al$_{17}$(Fe$_{3.2}$ Mn$_{0.8}$)$_3$Si$_2$ and β-Al$_5$FeSi are observed. Some complex particles are present in the alloys microstructure as the effect of incomplete peritectic reaction.
2. Electrical conductivity of the Al-Si-Mg alloys in the investigated range of chemical compositions is increasing with decreasing Si and Ti content and increasing Na content.
3. Ultimate tensile strength and yield strength are decreased by the addition of Si and Fe. Ti addition increase UTS of the investigated alloys.
4. Ductility of the Al-Si-Mg alloys is decreased by the

silicon addition and increased by the α-Al+β-Si eutectic mixture modification.

REFERENCES

[1] M.F. Ibrahim, E. Samuel, A.M. Samuel, A.M.A. Al-Ahmari, F.H. Samuel, Mater. Design. **32**, 2130-2142 (2011)

[2] S.G. Shabestari, Mat. Sci. Eng. A. **383**, 289-298 (2004)

[3] A. Fabrizi, S. Ferraro, G. Timelli, Mater. Charact. 85, 13–25 (2013).

[4] R. Fransiscus, A. Berkers, Arch. Foundry. Eng. 14, 5–8 (2005).

[5] M. Hajkowski, Ł. Bernat, J. Hajkowski, Arch. Foundry Eng. 12, 57–64 (2012).

[6] C.H. Caceres, I. L. Svensson, Int. J. Cast Met. Res. 15, 531–543 (2003).

[7] C. Ravi, Acta Mater. 52, 4213–4227 (2004).

[8] C.H. Caceres, C. J. Davidson, J. R. Griffiths, Q.G. Wang, Metall. Mater. Trans. A, 30, 2611–2618 (1999).

[9] H. Yang, S. Ji, W. Yang, Y. Wang, Z. Fan, Mater. Sci. Eng. A, 642, 340–350 (2015).

[10] A. Mamala, W. Sciężor, Arch. Metall. Mater. 59, 413-417 (2014).

[11] X. Cao, J. Campbell, Mater. Trans. 47, 1303–1312 (2006).

[12] N. Krendelsberger, F. Weitzer, J. C. Schuster, Metall. Mater. Trans. A, 38, 1681–1691 (2007).

[13] P. Ashtari, H. Tezuka, T. Sato, Scr. Mater. 53, 937–942 (2005).

[14] A. Gorny, J. Manickaraj, Z. Cai, S. Shankar, J. Alloys Compd., 577, 103–124 (2013).

[15] J.A. Taylor, Procedia Mater. Sci. 1, 19–33 (2012).

[16] O. Elsebaie, A.M.A. Mohamed, A.M. Samuel, F.H. Samuel, A.M.A. Al-Ahmari, Mater. Des. 32, 3205–3220 (2011).

[17] A.K. Dahle, K. Nogita, S.D. McDonald, C. Dinnis, L. Lu, Mater. Sci. Eng. A 413–414, 243–248 (2005).

[18] S. Hegde, K.N. Prabhu, J. Mater. Sci. 43, 3009–3027 (2008).

[19] S.A. Kori, B.S. Murty, M. Chakraborty, Mater. Sci. Eng. A 283, 94–104 (2000).

[20] B. Dybowski, B. Adamczyk-Cieślak, K. Rodak, I. Bednarczyk, A. Kiełbus, J. Mizera, Solid. State Phenom. 229, 3–10 (2015).

[21] M.V. Kral, Mater. Lett. 59, 2271–2276 (2005).

[22] Y. Choi, J. Lee, W. Kim, H. Ra, J. Mater. Sci. 4, 2163–2168 (1999).

[23] T. Rzychoń, A. Kiełbus, L. Lityńska-Dobrzyńska, Mater. Charact. 83, 21–34 (2013).

[24] M. Danaie, R.M. Asmussen, P. Jakupi, D. W. Shoesmith, G.A. Botton, Corros. Sci. 77, 151–163 (2013).

[25] M. Mulazimoglu, R. Drew, J. Gruzleski, Metall. Trans. A 20, 383–389 (1989).

[26] C.H. Cáceres, B.I. Selling, Mater. Sci. Eng. A 220, 109–116 (1996).